

Copper-Phosphido Catalysis: Enantioselective Coupling of Phosphines and Cyclopropenes

Brian S. Daniels,[‡] Xintong Hou,[‡] Stephanie A. Corio, Lindsey M. Weissman, Vy M. Dong,^{*} Jennifer S. Hirschi,^{*} Shaozhen Nie^{*}

Department of Chemistry, University of California, Irvine, Irvine, California 92697, United States

Department of Chemistry, Binghamton University, Binghamton, New York 13902, United States

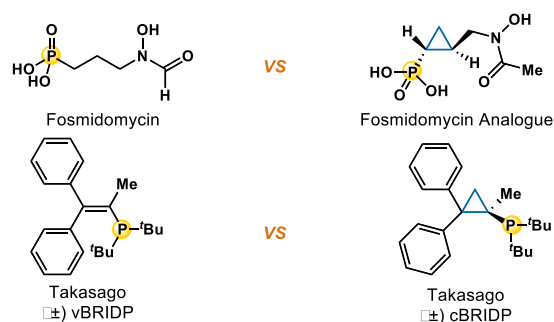
ABSTRACT: We describe a copper-catalyst that promotes the addition of phosphines to cyclopropenes at ambient temperature. A range of cyclopropylphosphines bearing different steric and electronic properties can now be accessed in high yields and enantioselectivities. A combined experimental and theoretical mechanistic study supports insertion of a Cu(I)-phosphido intermediate into the strained olefin. Density functional theory calculations reveal migratory insertion as the stereodetermining step of the pathway, with final product formation occurring via a *syn*-protodemetalation. Enrichment of phosphorus stereocenters is demonstrated via a DyKAT process.

By inventing strategies to forge C–P bonds, chemists enable rapid access to organophosphorous architectures for diverse applications in medicine and catalysis.¹ The cyclopropylphosphine motif attracts attention due to its unique steric and electronic profile. For example, a cyclic analogue of fosmidomycin shows enhanced antibiotic activity against *E. coli*, presumably due to restricted rotation.² In the realm of catalysis, Takasago's cyclopropyl phosphine ligand, cBRIDP outperforms its vBRIDP in Suzuki-Miyaura cross coupling; the cyclopropyl's electron-richness accelerates oxidative addition, while its sterics aid reductive elimination (Figure 1A).³ Considering ways to construct cyclopropyl phosphines, we focused on hydrophosphination: the direct addition of a P–H bond across a C=C multiple bond.⁴ Hydrophosphination represents an attractive and atom-economical platform⁵ for control of stereochemistry at carbon and/or phosphorous. While progress has been made, stereoselective methods remain rare.⁶ Further studies are warranted to extend additions beyond use of alkynes,⁷ oxa-bicycles,⁸ and Michael acceptors (Figure 1B).⁹ Driven by strain release,¹⁰ cyclopropenes show high reactivity in various applications.^{11,12} The hydrofunctionalization of cyclopropenes has enabled a direct access to a diverse range of enantiomerically enriched rings.¹²

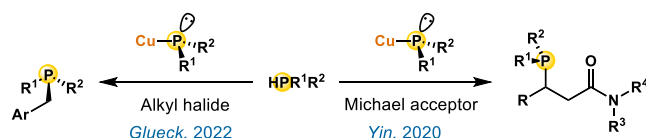
Organophosphorous partners bearing P–H bonds with a wide range of acidities (pKa 9.0 to 22.4) can be activated with transition metal-catalysts. Secondary phosphines lie at the upper end of this pKa range but are greatly acidified upon coordination to a transition metal. Deprotonation results in a metal-phosphido complex with high nucleophilicity, and recent studies have revealed impressive versatility of catalytically generated Cu-phosphido complexes. Glueck elucidated mechanistic and structural details, while Yin demonstrated catalytic transformations using Cu-phosphidos. Encouraged by these studies, we imagined using Cu-phosphido catalysis for the enantioselective hydrophosphination of cyclopropenes. Previous cyclopropene studies using both phosphine oxides and phosphites all gave ring-opening to

afford allylic phosphine oxides and allylic phosphonates. At the start of our studies, there was only one transformation, using phosphine oxides and cyclopropenes catalyzed by palladium which provided the ring-retained cyclopropyl phosphine product, albeit as a racemic mixture. Coinciding with our efforts, the Wang group was independently pursuing the enantioselective addition of phosphines to cyclopropenes by Pd-catalysis.

(A) Cyclopropyl phosphorus-containing molecules



(B) State of the art in Cu-phosphido reactivity



(C) Proposed asymmetric hydrophosphination of cyclopropene

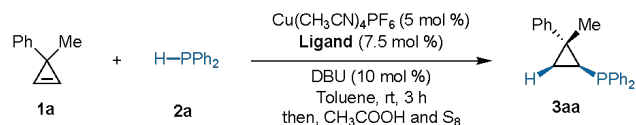


Figure 1. Inspiration for asymmetric hydrophosphination of cyclopropenes.

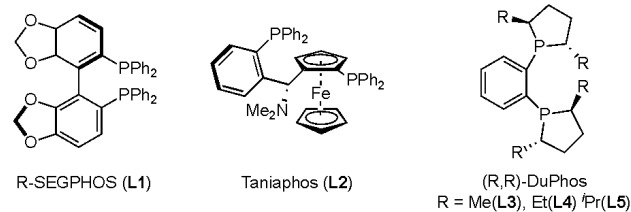
While promising, their scope is limited strictly to ester-bearing cyclopropenes and requires use of a precious metal. Herein, we report an enantioselective addition of phosphines to cyclopropenes via Cu-phosphido catalysis. Supported by detailed experimental and theoretical studies, we propose that

this complementary process occurs by the insertion of a phosphide intermediate into cyclopropenes. The protocol involves ambient temperatures and features the use of an earth abundant metal to access a wide range of cyclopropyl phosphines. Furthermore, we provide insights into ligand trends for selectivity on the basis of buried volume analysis.

Table 1. Ligand effects on asymmetric hydrophosphination of 1a^a



entry	variations	yield (%)	er
1	—	93	98:2
2	without Cu(CH ₃ CN)PF ₆	—	—
3	without DBU	—	—
4	no (R,R)-i-Pr-DuPhos	77	—
5	6 mol% ((R,R)-i-Pr-DuPhos	91	79:21
6	L1 instead of L5	90	85:15
7	L2 instead of L5	82	64:36
8	L3 instead of L5	70	90:10
9	L4 instead of L5	73	92:8



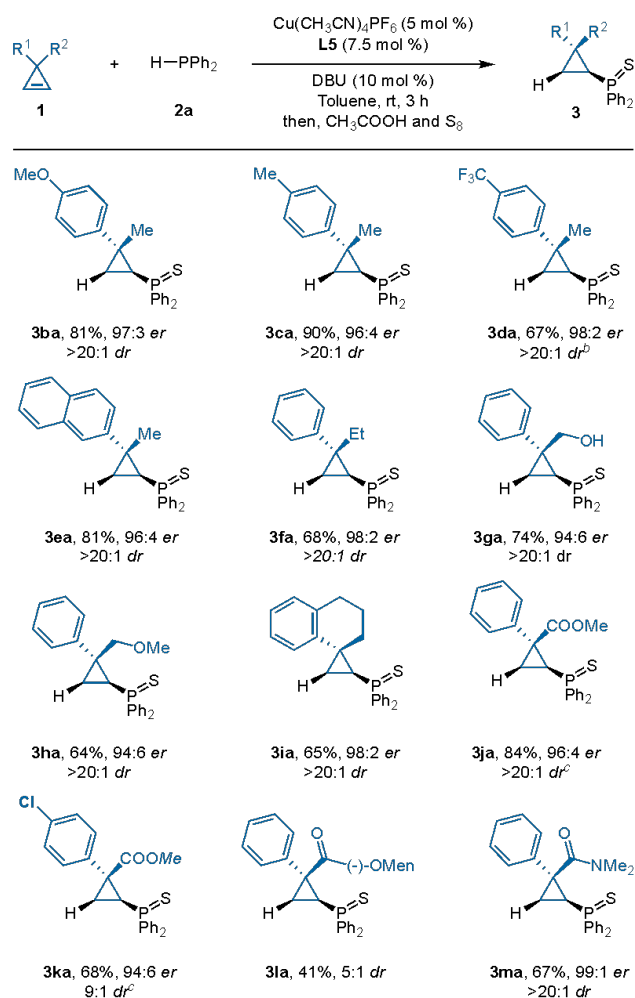
^aReaction conditions: 1a (0.12 mmol), 2a (0.10 mmol), Cu(CH₃CN)₄PF₆ (5.0 mol%), ligand (7.5 mol%), DBU (10 mol%), toluene (0.40 mL), 3 h. Yield determined by GC-FID analysis of the reaction mixture, which was referenced to 1,3,5-trimethoxybenzene internal standard. Enantioselectivity determined by chiral SFC.

In our initial studies, we surveyed phosphine oxides and found that it was difficult to achieve high enantioselectivity (Table xx SI). In contrast, diphenyl phosphine (2a) gave promising results with both Pd and Cu. Therefore, we choose diphenyl phosphine (2a) and cyclopropene 1a as model substrates. Although the Wang group reported that cyclopropene 1a does not transform under with their standard conditions,^{4g} we found that the SEGPPOS ligand family with Pd(OAc)₂ provides cyclopropyl phosphine 3aa in 86 % yield with 97:3 er (Table S1).¹⁸ In previous studies using copper catalysis, Yin's group has demonstrated the superiority of Taniaphos ligands for the Cu-catalyzed alkylation of secondary phosphines.^{9f} However, Taniaphos ligands were ineffective in this cyclopropene hydrophosphination (Table 1, entry 7). Instead, we found the DuPhos ligand family was most promising (Table 1, entry 8,9). Higher selectivity was correlated with larger R-substituents on the ligand (92% yield, 98:2 er). The addition of base is necessary to promote the formation of copper phosphido (Table 1, entry 3). With further tuning of the reaction stoichiometry, we developed a convenient and

practical protocol for the asymmetric coupling of phosphines and cyclopropenes.

Due to the unique structure of cyclopropyl phosphine compounds, the product is relatively air stable.³ For the convenience of handling and analysis, the cyclopropyl phosphine products were oxidized with sulfur to generate the corresponding phosphine sulfides. Compared to the scope of hydrophosphination developed by Wang group, we achieved a wider scope of 12 unique cyclopropene partners with different functionalities, electronics and sterics as summarized in Table 2.

Table 2. Hydrophosphination of various cyclopropenes.^a

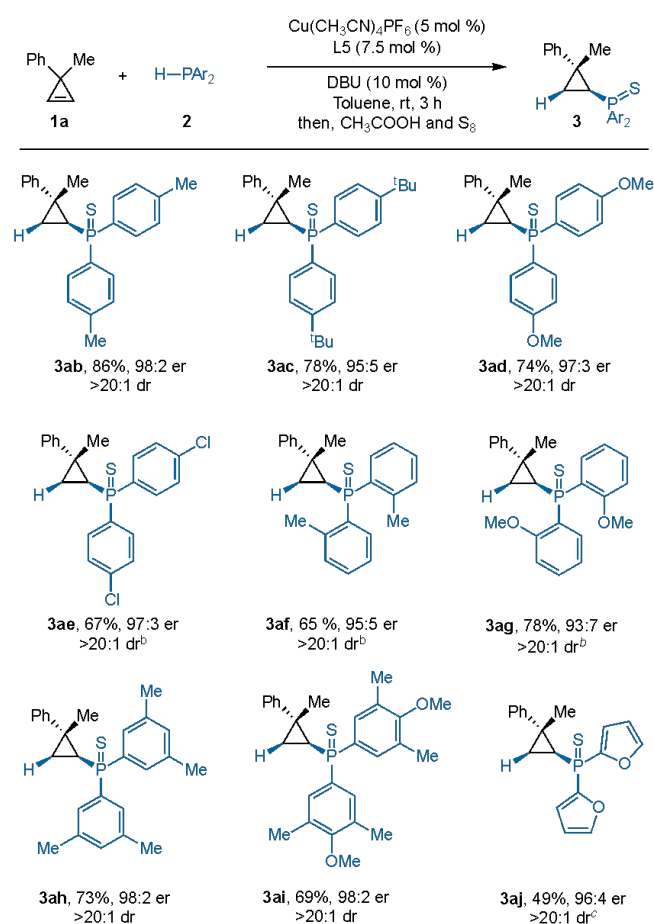


^aReaction conditions: **1** (0.12 mmol), **2a** (0.10 mmol), Cu(CH₃CN)₄PF₆ (5.0 mol%), ligand (7.5 mol%), DBU (10 mol%), toluene (0.40 mL), 3 h. Isolated yield of **3**. Diastereomeric ratios (*dr*) were determined from ¹H NMR analysis of the unpurified reaction mixture. Enantioselectivity determined by chiral SFC. ^bReaction time is 24 hours. ^cPd(OAc)₂ (5.0 mol%) and (R)-DM-SEGPPOS (6.0 mol%), 60 °C instead of standard condition, see SI for details.

Cyclopropenes with alcohol (**3ga**) and methyl ether (**3ha**) substituents undergo the transformation with moderate yields (64–74%) and high stereoselectivities (>20:1 *dr*, 94:6 er). Spiro compounds with quaternary carbons are common in natural products¹⁹ and are difficult to construct enantioselectively.²⁰ With this transformation, we successfully obtained hydrophosphinated tetralin (**3ia**) by desymmetrization of the

corresponding cyclopropene. Interestingly, ester cyclopropene **3ja** gives no enantioselectivity (50:50 *er*) with Cu standard condition, but high enantioselectivity was obtained by using Pd and DM-SEGPHOS. Therefore, cyclopropene **3ka** with *p*-Cl phenyl substituent was also desymmetrized using Pd and DM-SEGPHOS to provide corresponding cyclopropyl phosphine with moderate yield (68%) and stereoselectivity (9:1 *dr*, 94:6 *er*). The chlorine substituent provides an extra handle for further derivatization of the phosphine product. In addition, we desymmetrized menthol ester cyclopropene (**3la**) with moderate diastereoselectivity (5:1 *dr*). An amide substituted cyclopropene (**3ma**) also undergoes hydrophosphination with moderate yield (67%) and excellent stereoselectivity (>20:1 *dr*, 99:1 *er*).

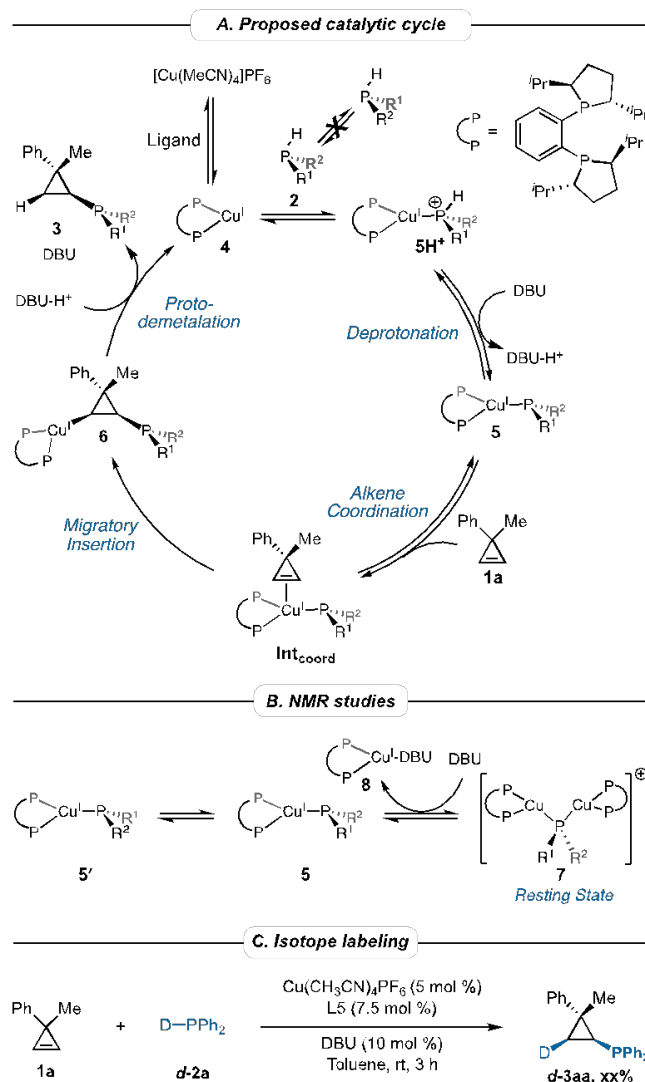
Table 3. Hydrophosphination of **1a** with various phosphines.^a



^aReaction conditions: **1** (0.12 mmol), **2a** (0.10 mmol), Cu(CH₃CN)₄PF₆ (5.0 mol%), ligand (7.5 mol%), DBU (10 mol%), toluene (0.40 mL), 3 h. Isolated yield of **3**. Diastereomeric ratios (*dr*) were determined from ¹H NMR analysis of the unpurified reaction mixture. Enantioselectivity determined by chiral SFC. ^bReaction performed for 12 hours. ^cReaction performed at 80 °C for 12 hours.

Our method also encompasses a range of different phosphine compounds and affords both good yields and stereoselectivity, as shown in Table 3. Phosphines bearing electron donating Me, *t*Bu, and OMe groups at the *para* position (**3ab**, **3ac**, **3ad**) show moderate to high yields (74–86

%) and high enantioselectivities (95:5–98:2 *er*). Electron poor phosphines are also well-tolerated (**3ae**). Even phosphines with *ortho* substituted (**3af**, **3ag**), 3,5-substituted (**3ah**) and 3,4,5-substituted aromatic rings (**3ai**) transform in 65–78% yield and high enantioselectivities (93:7–98:2 *er*). Our method additionally tolerates heterocyclic phosphines, such as 2-furyl **2j**, which gives **3aj** (49% yield, 96:4 *er*) at elevated temperature (80 °C, 12 hours).

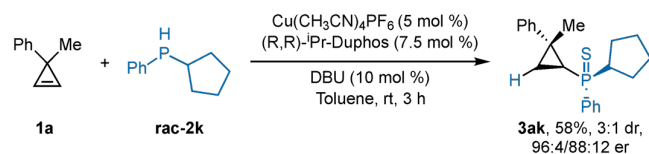


Scheme 1. A. Catalytic cycle for the asymmetric hydrophosphination of cyclopropenes via copper catalysis, as deduced from concurrent theoretical and experimental mechanistic findings. B. NMR identification of the off-cycle dimerization of monomeric Cu-phosphido complex. C. Isotope labeling experiment to probe stereoselectivity in hydrophosphination reaction.

Based on literature precedent^{9f,17d,17e} and our own observations, we propose the general catalytic cycle in Scheme 1. Initially, Cu(CH₃CN)₄PF₆ binds to (*R,R*)-*i*-Pr-DuPhos to generate a mono(chelate) species **4** followed by the monocoordination of phosphine (**2**) to generate copper phosphido complex **5**. In related studies, Glueck has proposed that the steric bulk of the ligand prevents coordination of the secondary phosphine to generate **5**.^{17d} Therefore, phosphine complexation coupled with deprotonation is a probable step

for the formation of **5**. A key step in the cycle involves addition of copper phosphido intermediate (**5**) to the cyclopropene (**1a**). We imagined that **5** could either undergo either direct nucleophilic attack²¹ or insertion into the cyclopropene π -bond.²² Lastly, elimination of the copper catalyst to regenerate **4** and release the final hydrophosphinated cyclopropane product **3** completes the catalytic cycle.

To investigate our proposed catalytic cycle (Scheme 1A), we performed a series of experimental mechanistic studies. Firstly, we studied the rate by variable time normalization analysis. We were surprised by the first order dependence of the DBU concentration and the fractional order dependence of the copper catalyst concentration on the reaction rate. In stark contrast to prior reports where addition of base to a mixture of $\text{Cu}(\text{CH}_3\text{CN})_4\text{PF}_6$, bidentate phosphine ligand, and secondary phosphine results in a complicated mixture, our ³¹P NMR data shows immediate and clean formation of a new species, which we have characterized as a Cu-phosphido dimer **7** (Scheme 1B), where the lone pair of the X-type phosphido ligand of **5** acts as an L-type ligand to form a $\left[2\right]$ bridge to another unit of Cu-DuPhos mono-chelate **4** via a three-center four-electron bond. We propose this species to be the catalyst resting state due to its persistence and remarkable stability under reaction conditions. In line with this observation, our kinetics studies, and similar observations made by Appel and coworkers while studying copper hydride catalysis,²³ we propose the DBU acts as not only a base but also an L-type ligand. The DBU undergoes ligand substitution with the dimeric resting state **7** to liberate the catalytically active monomeric copper phosphide **5**. This hypothesis is further supported by ³¹P NMR studies which reveal decomposition of the dimer **7** with concomitant formation of an unidentified species in the presence of large excesses of DBU. Finally, the reaction performed with *d*-**2a** revealed that the hydrophosphination proceeds via a formal syn-addition of the P-H bond across the cyclopropene double bond (Scheme 1C).²⁴



Scheme 2. Dynamic kinetic asymmetric transformation.

With this mechanism in mind, we examined the possibility of setting a phosphorus stereocenter via a dynamic kinetic asymmetric transformation (DyKAT).²⁵ As outlined in the proposed mechanism, pyramidal inversion of the secondary phosphine is impractically slow at room temperature while epimerization of copper phosphido **5** with **5'** occurs rapidly.²⁶ We subjected asymmetrically substituted phosphine **2k** to the reaction conditions to test this hypothesis and observed a 3:1 *dr* for the inseparable cyclopropyl phosphine products with *er* of 96:4 and 88:12 respectively (Scheme 2). Based on our prior results, we assume desymmetrization of the cyclopropene is achieved effectively but with low control over the configuration of the phosphorus stereocenter, in line with a recent report from Glueck using a similar catalyst system for asymmetric alkylation of secondary phosphines.^{17d,17e} A dimeric resting state was again observed by ³¹P NMR studies of phosphine **2k**, thwarting attempts to compare the *dr* of the monomeric copper phosphido catalyst to the Curtin-Hammett controlled product distribution.

To support the proposed mechanism and elucidate a detailed pathway for the enantioselective hydrophosphination of cyclopropenes, we performed a density functional theory (DFT) analysis on the title reaction of 3-methyl-3-phenylcyclopropene (**1a**) and diphenylphosphine (**2a**) catalyzed by copper-*i*-Pr-DuPhos complex (**4**). DFT computations were performed utilizing $\omega\text{B97XD/def2TZVP PCM}(\text{toluene})//\text{B97D/def-2SVP}$ level of theory as implemented in Gaussian 16.²⁷⁻³³ Thermal corrections were computed using Grimme's quasi-rigid rotor harmonic oscillator approximation.³⁴ IRC calculations were performed to confirm that transition structures (TSs) connected minima along the potential energy surface. A thorough exploration of the catalyst conformational space was performed using CREST. In addition, a detailed exploration of TS conformations was performed for the selectivity-determining step (see Supporting Information page S5 for details)

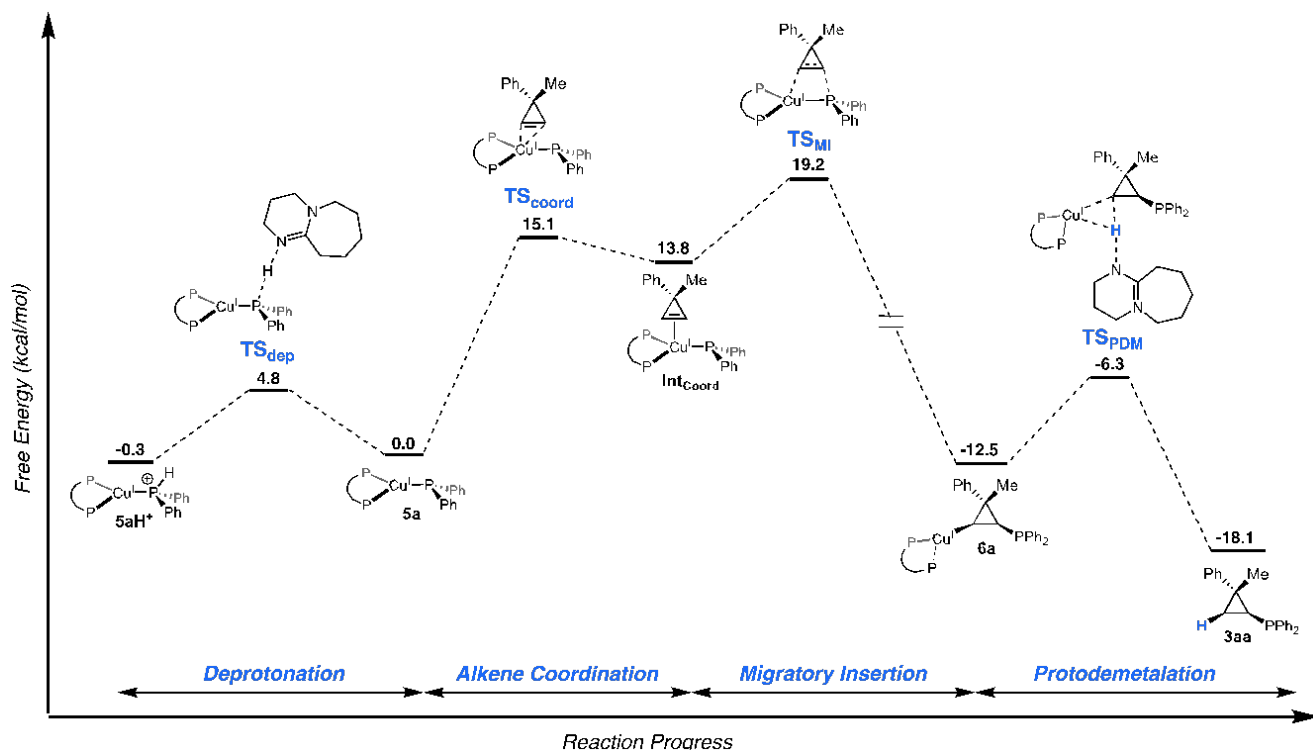


Figure 2. Reaction coordinate diagram depicting the relative barriers of deprotonation, alkene coordination, migratory insertion and protodemetalation in the hydrophosphination of cyclopropene. Migratory insertion is the stereoselectivity determining step.

Our computational study sought to identify both the turnover-limiting and stereoselectivity-determining steps of the catalytic cycle and to explain the origins of experimentally observed stereoselectivity. The potential energy surface for the lowest energy pathway resulting from our investigation is shown in Figure 2. The reaction is initiated via the coordination of diphenyl phosphine **2a** to Cu-Duphos to give the Cu-HPPH₂⁺ complex **5aH**⁺. Deprotonation of this cationic complex **5aH**⁺ by DBU is a low barrier step (**TS**_{dep}, $\Delta G^\ddagger = 4.8$ kcal/mol) that leads to the reversible formation of Cu-phosphido intermediate **5a** (chosen as the reference structure in the reaction coordinate). Following deprotonation, **5a** binds cyclopropene **1a** via π -coordination transition structure **TS**_{coord} ($\Delta G^\ddagger = 15.1$ kcal/mol) to generate Cu-alkene complex **Int**_{Coord}. The subsequent 1,2-migratory insertion into the cyclopropene π -bond (**TS**_{MI}) has a free energy barrier of 19.2 kcal/mol relative to **5a** and represents a highly exothermic step in the pathway, which results in a stable, significantly lower energy copper coordinated cyclophosphinated intermediate **6a** – residing 12.5 kcal/mol below the monomeric resting state **5a**. The reaction pathway then proceeds through a facile stereoretentive protodemetalation (**TS**_{PDM}, $\Delta G^\ddagger = -6.3$ kcal/mol relative to **5a**) – a copper mediated protonation from DBU occurs *syn* to the diphenylphosphine substituent – to concomitantly regenerate **4** and afford the *syn*-hydrophosphinated cyclopropene product **3aa** (transferred proton shown in blue).^{35–37} This protodemetalation step (**TS**_{PDM}) proceeds through a unique three-center, two-electron bond transition structure (C–Cu bond-breaking is 2.11 Å and C–H bond forming distance is 1.42 Å), consistent with the exclusive *syn* addition observed when the reaction is performed with *d*-**2a** (Figure 3 and Scheme 1c) (vide supra). Incidentally, several alternative pathways for protodemetalation were also

explored computationally (See Supporting Information page S6). A *syn*-protodemetalation TS analogous to **TS**_{PDM}, whereby copper mediates the proton transfer from a protonated PPH₂ on the adjacent carbon, was found to be 25 kcal/mol higher in energy than **TS**_{PDM}.

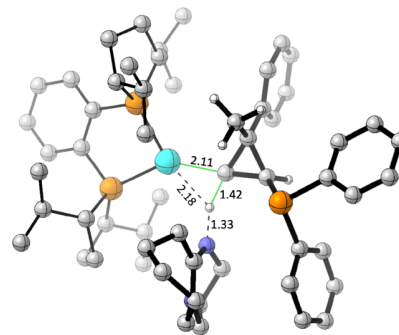


Figure 3. Three-center, two-electron bond transition structure for the product-forming *syn*-protodemetalation of Cu-Duphos from cyclopropene via DBU-H⁺.

Analysis of the potential energy surface indicates that **TS**_{MI} is the enantio- and diastereoselectivity-determining step in the hydrophosphination reaction. To investigate catalyst-substrate interactions that dictate the enantioselectivity in this reaction, a conformational search was conducted on **TS**_{MI} for transition structures that lead to the formation of both the major and minor enantiomers of **3aa**. The lowest energy transition structure which leads to the major enantiomer (Figure 4A, **TS**_{MI-Major}) is favored by 2.1 kcal/mol with respect to the lowest energy structure for the minor enantiomer (Figure 4A, **TS**_{MI-Minor}). At 298 K, a $\Delta\Delta G^\ddagger$ of 2.1 kcal/mol corresponds to a predicted *er* of 97.5:2.5, which is in excellent agreement with

the experimental *er* of 98:2 ($\Delta\Delta G^\ddagger$ of 2.3 kcal/mol) for the title reaction.

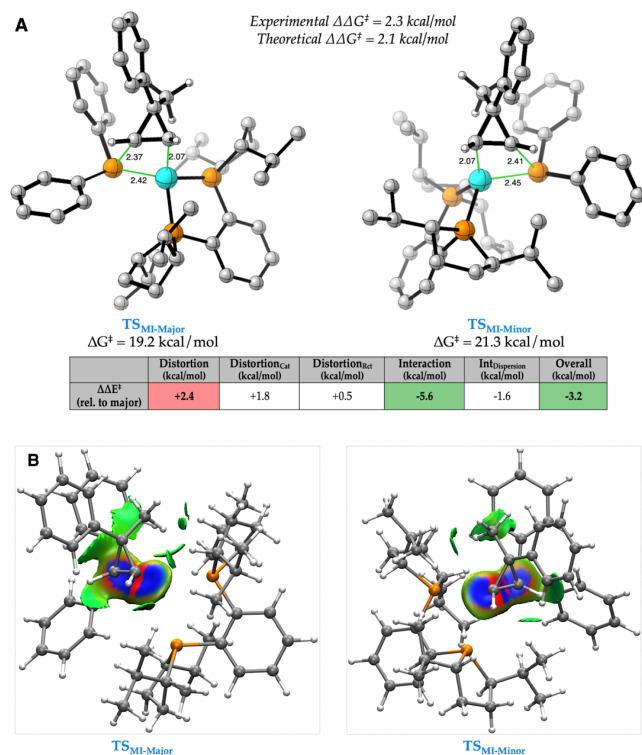


Figure 4. (A) Lowest energy TSs of the enantioselectivity-determining step with experimental and theoretical free energy barriers after Boltzmann weighting. Also shown are components of the energy decomposition analysis relative to the major enantiomer. Δ Distortion of the catalyst (Cat) and reactants (Rct) versus overall Δ Interaction (including Δ Dispersion) are highlighted. (B) Non-covalent interaction (NCI) plots depict dispersive interactions (shown in green) between Cu-DuPhos and PPh₂ with cyclopropene reactants for each TS leading to the major and minor enantiomers of product (Isosurface of 0.009).

To further evaluate the origin of enantioselectivity, a distortion-interaction analysis was performed on TS_{MI-Major} and TS_{MI-Minor}.³⁸⁻⁴⁰ Distortion energy describes the energy required to distort reactants and catalysts from their respective ground states into the necessary transition state conformations. Energy decomposition revealed that the major enantiomer suffers a greater degree of distortion energy, 2.4 kcal/mol ($\Delta\Delta E^\ddagger$) more than the minor enantiomer (Figure 4A). The majority (1.8 kcal/mol) of this 2.4 kcal/mol difference in distortion energy arises from the distortion of the diphenyl phosphine and Cu-DuPhos catalyst, while the remaining 0.6 kcal/mol arises from distortion of the cyclopropene substrate. Despite distortion energy favoring the minor enantiomer, advantageous interaction energy favors the major enantiomer by 5.6 kcal/mol. Interaction energy describes how the distorted catalyst and reactant fragments interact with one another within the TS, a portion of this can be accounted for as dispersion energy. The major enantiomer exhibits favorable dispersions in the form of significant CH— π interactions between the diphenylphosphine and the cyclopropene methyl group as well as moderate dispersions amongst the Cu-DuPhos isopropyl groups and the cyclopropene substrate (Figure 4B). A visual comparison of the dispersion interactions in the enantioselectivity-determining transition states shows that

TS_{MI-Major} enjoys more stabilizing dispersion interactions than TS_{MI-Minor} (as evidenced by the greater green areas in the NCI plots of the two TSs shown in Figure 4B).^{41,42} In addition to the favorable dispersions imparted by its isopropyl groups in TS_{MI-Major}, the Cu-DuPhos catalyst also serves to add steric bulk to the catalytic pocket, blocking more than three-fourths of the pocket when coordinated to PPh₂, forcing the cyclopropene substrate to bind in the same location for both enantiomers (see Supporting Information page C9).

From this analysis, steric interactions have been identified to play a key role in controlling stereoselectivity. Using this information, we chose to investigate the buried volume and steric maps for intermediate **5a** with **L1**, **L3**, **L4** and **L5** as ligands.⁴³⁻⁴⁴ The buried volume analysis reveals that ligand **L1** (Figure 5A) has a slightly smaller available free volume compared to the best ligand **L5** (Figure 5C). However, **L5** is more fluxional compared to the rigid biphenyl backbone of **L1**, thereby accommodating the incoming cyclopropene more readily. This leads to an overall reduction in the background reaction of **L5**, compared to **L1**, thus enabling better enantioselectivity in **L5**. Similarly, despite having the same backbone as **L5** (R=iPr), ligands **L3** (R=Me, Figure 5B) and **L4** (R=Et) have more available free volume, leading to overall poorer steric control and slightly lower enantioselectivity.⁴⁵

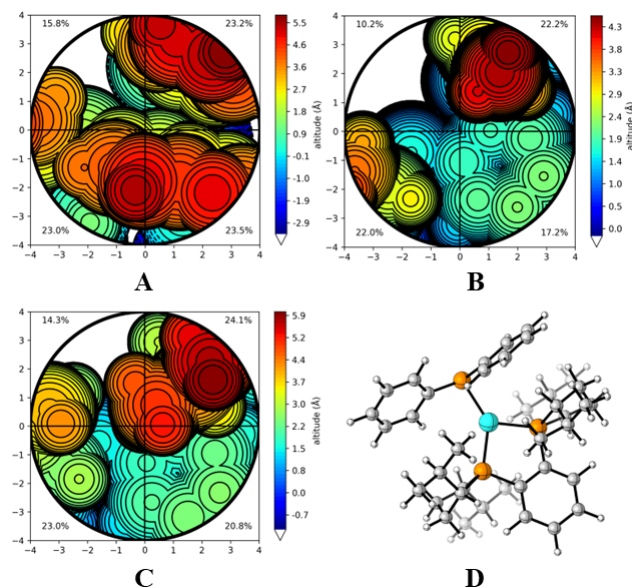


Figure 5. Steric maps depicting the catalytic pocket prior to coordination of cyclopropene when the ligand on copper is (A) R-SEGPHOS (**L1**), (B) (R,R)-Me-DuPhos (**L3**), or (C) (R,R)-iPr-DuPhos (**L5**). The orientation of the copper-phosphido complexes in these steric maps is depicted in D.

In conclusion, we report asymmetric hydrophosphination of cyclopropenes in high enantio- and diastereoselectivities. Mechanistic studies reveal an unusual dimeric resting state and a surprising rate enhancement effect from DBU, which plays an important role in forming the catalytically active monomer. Enrichment of phosphorus stereocenters is additionally demonstrated through a DyKAT of an unsymmetrically substituted secondary phosphine. Both the enantio- and diastereoselectivity of the product is determined during the migratory insertion step. An analysis of the relevant

TSs indicate that selectivity is controlled by a combination of dispersion and steric interactions. Future studies will focus on achieving higher control of this phosphorus stereocenter and elaborating the cyclopropyl phosphine products to afford mono- or bidentate phosphine ligands. We expect insight from these studies to guide the development of related strategies in copper catalysis, hydrofunctionalization, and phosphine synthesis.

ASSOCIATED CONTENT

Supporting Information

(Word Style "TE_Supporting_Information"). (Word Style "TE_Supporting_Information"). A listing of the contents of each file supplied as Supporting Information should be included. For instructions on what should be included in the Supporting Information as well as how to prepare this material for publication, refer to the journal's Instructions for Authors.

The Supporting Information is available free of charge on the ACS Publications website.

brief description (file type, i.e., PDF)

brief description (file type, i.e., PDF)

AUTHOR INFORMATION

Corresponding Authors

Vy M. Dong – Department of Chemistry, University of California, Irvine, Irvine, California 92697, United States; orcid.org/0000-0002-8099-1048; Email: dongv@uci.edu

Jennifer S. Hirschi – Department of Chemistry, Binghamton University, Binghamton, New York 13902, United States; <https://orcid.org/0000-0002-3470-0561>; Email: jhirschi@binghamton.edu

Shaozhen Nie – Department of Medicinal Chemistry, GSK, 1250 South Collegeville Road, Collegeville, Pennsylvania 19426, United States; Email: shaozhen.x.nie@gsk.com

Authors

Brian S. Daniel – Department of Chemistry, University of California, Irvine, Irvine, California 92697, United States

Xintong Hou – Department of Chemistry, University of California, Irvine, Irvine, California 92697, United States

Stephanie A. Corio – Department of Chemistry, Binghamton University, Binghamton, New York 13902, United States; <https://orcid.org/0000-0001-9029-3895>

Lindsey M. Weissman – Department of Chemistry, Binghamton University, Binghamton, New York 13902, United States; <https://orcid.org/0000-0003-4437-9991>

Author Contributions:

‡ Brian S. Daniel and Xintong Hou contributed equally to this work.

Funding Sources

VMD acknowledges the National Science Foundation (CHE-1956457). JSH acknowledges the National Institute of General Medicine NIH R35GM147183 as well as the XSEDE Science Gateway Program (under the NSF Grant Numbers ACI-1548562, CHE180061).

Notes

Any additional relevant notes should be placed here.

ACKNOWLEDGMENT

(Word Style "TD_Acknowledgments"). Generally the last paragraph of the paper is the place to acknowledge people (dedications), places, and financing (you may state grant numbers and sponsors here). Follow the journal's guidelines on what to include in the Acknowledgement section.

ABBREVIATIONS

CCR2, CC chemokine receptor 2; CCL2, CC chemokine ligand 2; CCR5, CC chemokine receptor 5; TLC, thin layer chromatography.

REFERENCES

- [1] (a) Zhou, Q.-L. *Privileged Chiral Ligands and Catalysts*; Wiley-VCH: Weinheim, Germany, 2011; Vol. 6. (b) Horsman, G. P.; Zechel, D. L. Phosphonate Biochemistry. *Chem. Rev.* **2017**, *117*, 5704–5783. (c) Ni, H.-Z.; Chan, W.-L.; Lu, Y.-X. Phosphine-Catalyzed Asymmetric Organic Reactions. *Chem. Rev.* **2018**, *118*, 9344–9411. (d) Iaroshenko, V.; *Organophosphorus Chemistry: from Molecules to Applications*. Wiley-VCH: Weinheim, **2019**.
- [2] Devreux, V.; Wiesner, J.; Goeman, J. L.; Van der Eycken, J.; Jomaa, H.; Van Calenbergh, S. Synthesis and Biological Evaluation of Cyclopropyl Analogues of Fosmidomycin as Potent *Plasmodium falciparum* Growth Inhibitors. *J. Med. Chem.* **2006**, *49*, 2656–2660.
- [3] Suzuki, K.; Hori, Y.; Nakayama, Y.; Kobayashi, T. Development of New Phosphine Ligands (BRIDPs) for Efficient Palladium-Catalyzed Coupling Reactions and Their Application to Industrial Process. *J. Synth. Org. Chem.*, **2011**, *69*, 1231–1240.
- [4] (a) Wicht, D. K.; Glueck, D. S. *Hydrophosphination and Related Reactions*. Togni, A.; Grützmacher, H.; Eds.; Wiley-VCH: Weinheim, **2001**; pp 143–170. (b) Rosenberg, L. Mechanism of Metal-Catalyzed Hydrophosphination of Alkenes and Alkynes. *ACS Catal.* **2013**, *3*, 2845–2855. (c) Bange, C. A.; Waterman, R. Challenges in Catalytic Hydrophosphination. *Chem. – Eur. J.* **2016**, *22*, 12598–12605. (d) Glueck, D. S. Metal-Catalyzed P-C Bond Formation via P-H Oxidative Addition: Fundamentals and Recent Advance. *J. Org. Chem.* **2020**, *85*, 14276–14285. (e) Troev, K. D.; Reactivity of P-H Group of Phosphines. *Academic Press*, **2018**, 19–144. (f) Belli, R. G.; Yang, J.; Bahena, E. N.; McDonald, R.; Rosenberg, L. Mechanism and Catalyst Design in Ru-Catalyzed Alkene Hydrophosphination. *ACS Catal.* **2022**, *12*,

- 5247–5246. (f) Novas, B.; Waterman, R. Metal-Catalyzed Hydrophosphination. *ChemRxiv* **2022**, [10.26434/chemrxiv-2022-1thn2](https://doi.org/10.26434/chemrxiv-2022-1thn2). (g) Zhang, Y.; Jiang, Y.; Li, M.; Huang, Z.; Wang, J. Palladium-catalyzed diastereoselective desymmetric hydrophosphination of cyclopropenes. *Chem. Cat.*, **2022**, *2*, 1–11.
- [5] Trost, B. M. The Atom Economy—A Search for Synthetic Efficiency. *Science* **1991**, *254*, 1471–1477.
- [6] (a) Pullarkat, S. A.; Leung, P.-H. Chiral Metal Complex-Promoted Asymmetric Hydrophosphination. *Top. Organomet. Chem.* **2011**, *43*, 145–166. (b) Pullarkat, S.A. Recent Progress in Palladium-Catalyzed Asymmetric Hydrophosphination. *Synthesis* **2016**, *48*, 493–503. (c) Chew, R. J.; Leung, P.-H. Our Odyssey with Functionalized Chiral Phosphines: From Optical Resolution to Asymmetric Synthesis to Catalysis. *Chem. Rec.* **2016**, *16*, 141–158.
- [7] (a) Join, B.; Mimeau, D.; Delacroix, O.; Gaumont, A. C.; Pallado-catalyzed hydrophosphination of alkynes: access to enantio-enriched P-stereogenic vinyl phosphine-boranes. *Chem. Commun.* **2006**, *30*, 3249–3251. (b) Liu, X.-T.; Han, X.-Y.; Wu, Y.; Sun, Y.-Y.; Gao, L.; Huang, Z.; Zhang, Q.-W. Ni-Catalyzed Asymmetric Hydrophosphination of Unactivated Alkynes. *J. Am. Chem. Soc.* **2021**, *143*, 11309–11316.
- [8] (a) Sadler, A.; Ong, Y. J.; Kojima, T.; Foo, C. Q.; Li, Y.; Pullarkat, S. A.; Leung, P.-H. Desymmetrization of Achiral Heterobicyclic Alkenes through Catalytic Asymmetric Hydrophosphination. *Chem. – Asian J.* **2018**, *13*, 2829–2833. (b) Lu, Z.-W.; Zhang, H.-Y.; Yang, Z.-P.; Ding, N.; Meng, L.; Wang, J. Asymmetric Hydrophosphination of Heterobicyclic Alkenes: Facile Access to Phosphine Ligands for Asymmetric Catalysis. *ACS Catal.* **2019**, *9*, 1457–1463.
- [9] (a) Kovacic, I.; Wicht, D. K.; Grewal, N. S.; Glueck, D. S.; Incarvito, C. D.; Guzei, I. A.; Rheingold, A. L. Pt(Me-Duphos)-Catalyzed Asymmetric Hydrophosphination of Activated Olefins: Enantioselective Synthesis of Chiral Phosphines. *Organometallics* **2000**, *19*, 950–953. (b) Sadow, A. D.; Haller, I.; Fadini, L.; Togni, A. Nickel(II)-Catalyzed Highly Enantioselective Hydrophosphination of Methacrylonitrile. *J. Am. Chem. Soc.* **2004**, *126*, 14704–14705. (c) Feng, J.-J.; Chem, X.-F.; Shi, M.; Duan, W.-L. Palladium-Catalyzed Asymmetric Addition of Diarylphosphines to Enones toward the Synthesis of Chiral Phosphines. *J. Am. Chem. Soc.* **2010**, *132*, 5562–5563. (d) Huang, Y.-H.; Pullarkat, S. A.; Li, Y.-X.; Leung, P. H. Palladacycle-Catalyzed Asymmetric Hydrophosphination of Enones for Synthesis of C* and P* Chiral Tertiary Phosphines. *Inorg. Chem.* **2012**, *51*, 2533–2540 (d) Chen, Y.-R.; Feng, J.-J.; Duan, W.-L. NHC-copper-catalyzed asymmetric 1,4-addition of diarylphosphines to α,β -unsaturated ketones. *Tetrahedron Lett.*, **2014**, *55*, 595–597. (e) Teo, R. H. X.; Chen, H. G. J.; Li, Y.-X.; Pullarkat, P. A.; Leung, P. K. Asymmetric Catalytic 1,2-Dihydrophosphination of Secondary 1,2-Diphosphines Direct Access to Free P* and P*, C*-Diphosphines. *Adv. Synth. Catal.* **2020**, *362*, 2373–2378. (f) Li, Y.-B.; Tian, H.; Yin, L. Copper(I)-Catalyzed Asymmetric 1,4-Conjugate Hydrophosphination of α,β -Unsaturated Amides. *J. Am. Chem. Soc.* **2020**, *142*, 20098–20106. (g) Yue, W.-J.; Xiao, J.-Z.; Zhang, S.; Yin, L. Rapid Synthesis of Chiral 1,2-Bisphosphine Derivatives through Copper(I)-Catalyzed Asymmetric Conjugate Hydrophosphination. *Angew. Chem. Int. Ed.* **2020**, *59*, 7057–7062. (h) Wang, C.-Y.; Huang, K.-S.; Ye, J.; Duan, W.-L. Asymmetric Synthesis of P-Stereogenic Secondary Phosphine-Boranes by an Unsymmetric Bisphosphine Pincer-Nickel Complex. *J. Am. Chem. Soc.* **2021**, *143*, 5685–5690. (i) Pérez, J. M.; Postolache, R.; Castiñeira Reis, M.; Sinnema, E. G.; Vargová, D.; Vries, F.; Otten, E. Ge, L.; Harutyunyan, S. R. Manganese(I)-Catalyzed H-P Bond Activation via Metal-Ligand Cooperation. *J. Am. Chem. Soc.* **2021**, *143*, 20071–20076. (j) Ge, L.; Harutyunyan, S. R. Manganese(I)-Catalyzed Access to 1,2-Bisphosphine Ligands. *Chem. Sci.*, **2022**, *13*, 1307–1312.
- [10] (a) Bach, R. D.; Dmitrenko, O. Strain Energy of Small Ring Hydrocarbons. Influence of C-H Bond Dissociation Energies. *J. Am. Chem. Soc.* **2004**, *126*, 4444–4452. (b) Kenneth B. Wiberg, The Concept of Strain in Organic Chemistry. *Angew. Chem. Int. Ed.* **1986**, *25*, 312–322.
- [11] (a) Demjanov, N. Y.; Doyarenko, M. N. Cyclopropene. *Bull. Acad. Sci. Russ.* **1922**, *16*, 297–304. (b) Carter, F. L.; Frampton, V. L. Review of the chemistry of cyclopropene compounds. *Chem. Rev.* **1964**, *64*, 497–525. (c) Closs, G. L. Cyclopropenes. *Adv. Alicyclic Chem.* **1966**, *1*, 53–127. (d) Baird, M. S. Thermally induced cyclopropene-carbene rearrangements: an overview. *Chem. Rev.* **2003**, *103*, 1271–1294. (e) Walsh, R. The cyclopropene pyrolysis story. *Chem. Soc. Rev.* **2005**, *34*, 714–732. (f) Rubín, M.; Rubina, M.; Gevorgyan, V. Recent advances in cyclopropene chemistry. *Synthesis* **2006**, *2006*, 1221–1245. (g) Rubín, M.; Rubina, M.; Gevorgyan, V. Transition metal chemistry of cyclopropenes and cyclopropanes. *Chem. Rev.* **2007**, *107*, 3117–3179. (h) Zhu, Z.-B.; Wei, Y.; Shi, M. Recent developments of cyclopropene chemistry. *Chem. Soc. Rev.* **2011**, *40*, 5534–5563. (i) Vicente, R. Recent progresses towards the strengthening of cyclopropene chemistry. *Synthesis* **2016**, *48*, 2343–2360. (j) Raiguru, B. P.; Nayak, S.; Mishra, D. R.; Das, T.; Mohapatra, S.; Mishra, N. P. Synthetic Applications of Cyclopropene and Cyclopropenone: Recent Progress and Developments. *Asian J. Org. Chem.* **2020**, *9*, 1088–1132. (k) Li, P.-H.; Zhang, X.-Y.; Shi, M. Recent developments in cyclopropene chemistry. *Chem. Commun.* **2020**, *56*, 5457–5471. (l) Cohen, Y.; Marek, I. Regio- and Diastereoselective Copper Catalyzed Carbometallation of Cyclopropenylsilanes. *Org. Lett.* **2019**, *21*, 9162–9165.
- [12] (a) Dian, L.-Y.; Marek, I. Asymmetric Preparation of Polysubstituted Cyclopropanes Based on Direct Functionalization of Achiral Three-Membered Carbocycles. *Chem. Rev.* **2018**, *118*, 8415–8434. (b) Rubina, M.; Rubín, M.; Gevorgyan, V. Catalytic Enantioselective Hydroboration of Cyclopropenes. *J. Am. Chem. Soc.* **2003**, *125*, 7198–7199. (c) Rubina, M.; Rubín, M.; Gevorgyan, V. Catalytic Enantioselective Hydrostannation of Cyclopropenes. *J. Am. Chem. Soc.* **2004**, *126*, 3688–3689. (d) Sherrill, W. M.; Rubín, M. Rhodium-Catalyzed Hydroformylation of Cyclopropenes. *J. Am. Chem. Soc.* **2008**, *130*, 13804–13809. (e) Phan, D. H. T.; Kou, K. G. M.; Dong, V. M. Enantioselective Desymmetrization of Cyclopropenes by Hydroacylation. *J. Am. Chem. Soc.* **2010**, *132*, 16354–16355. (f) Liu, F.; Bugaut, X.; Schedler, M.; Fröhlich, R.; Glorius, F. Designing N-Heterocyclic Carbenes: Simultaneous Enhancement of Reactivity and Enantioselectivity in the Asymmetric Hydroacylation of Cyclopropenes. *Angew. Chem., Int. Ed.* **2011**, *50*, 12626–12630. (g) Teng, H.-L.; Luo, Y.; Wang, B.; Zhang, L.; Nishiura, M.; Hou, Z. Synthesis of Chiral Aminocyclopropanes by Rare-Earth-Metal Catalyzed Cyclopropene Hydroamination. *Angew. Chem., Int. Ed.* **2016**, *55*, 15406–15410. (h) Parra, A.; Amenós, L.; Guisán-Ceinos, M.; López, A.; Ruano, J. L. G.; Tortosa, M. Copper-Catalyzed Diastereo- and Enantioselective Desymmetrization of Cyclopropenes: Synthesis of Cyclopropylboronates. *J. Am. Chem. Soc.* **2014**, *136*, 15833–15836. (i) Li, Z.; Zhao, J.; Sun, B.; Zhou, T.; Liu, M.; Liu, S.; Zhang, M.; Zhang, Q. Asymmetric Nitrene Synthesis via Ligand-Enabled Copper-Catalyzed Cope-Type Hydroamination of Cyclopropene with Oxime. *J. Am. Chem. Soc.* **2017**, *139*, 11702–11705. (j) Luo, Y.; Teng, H.-L.; Nishiura, M.; Hou, Z. Asymmetric Yttrium-Catalyzed C(sp³)-H Addition of 2-Methyl Azaarenes to Cyclopropenes. *Angew. Chem., Int. Ed.* **2017**, *56*, 9207–9210. (k) Dian, L.; Marek, I. Rhodium-Catalyzed Arylation of Cyclopropenes Based on Asymmetric Direct Functionalization of Three Membered Carbocycles. *Angew. Chem., Int. Ed.* **2018**, *57*, 3682–3686. (l) Zhang, H.; Huang, W.; Wang, T.; Meng, F.-K. Cobalt Catalyzed Diastereo- and Enantioselective Hydroalkenylation of Cyclopropenes with Alkenylboronic Acids. *Angew. Chem., Int. Ed.* **2019**, *58*, 11049–11053. (m) Zheng, G.-F.; Zhou, Z.; Zhu, G.-X.; Zhai, S.-L.; Xu, H.-Y.; Duan, X.-J.; Yi, W.; Li, X.-W. Rhodium(III)-Catalyzed Enantio- and

Diastereoselective C-H Cyclopropylation of N-Phenoxy-sulfonamides: Combined Experimental and Computational Studies. *Angew. Chem., Int. Ed.* **2020**, *59*, 2890–2896 (n) Huang, W.; Meng, F.-K. Cobalt-Catalyzed Diastereo- and Enantioselective Hydroalkylation of Cyclopropenes with Cobalt Homo-enolates. *Angew. Chem., Int. Ed.* **2021**, *59*, 2694–2698. (o) Dian, L.; Marek, I. Cobalt-Catalyzed Diastereoselective and Enantioselective Hydrosilylation of Achiral Cyclopropenes. *Org. Lett.* **2020**, *22*, 4914–4918. (p) Nie, S.-Z.; Lu, A.; Kuker, E. L.; Dong, V. M. Enantioselective Hydrothiolation: Diverging Cyclopropenes through Ligand Control. *J. Am. Chem. Soc.* **2021**, *143*, 6176–6184. (q) Yu, R.; Cai, S.-Z.; Li, C.; Fang, X. Nickel-Catalyzed Asymmetric Hydroxyloxy- and Hydroalkoxycarbonylation of Cyclopropenes. *Angew. Chem., Int. Ed.* **2022**, doi.org/10.1002/anie.202200733. (r) Huang, Q.; Chen, Y.; Zhou, X.; Dai, L.; Lu, Y. Nickel-Hydride-Catalyzed Diastereo- and Enantioselective Hydroalkylation of Cyclopropenes. *Angew. Chem. Int. Ed.*, **2022**.

[13] Li, J.-N.; Liu, L.; Fu, Y.; Guo, Q.-X. What are the pKa values of organophosphorus compounds? *Tetrahedron* **2006**, *62*, 4453–4462.

[14] (a) Han, L.-B.; Zhao, C.-Q.; Onozawa, S.; Goto, M.; Tanaka, M. Retention of configuration on the oxidative addition of P-H bond to platinum(0) complexes: the first straightforward synthesis of enantiomerically pure P-chiral alkenylphosphinates via palladium-catalyzed stereospecific hydrophosphinylation of alkynes. *J. Am. Chem. Soc.* **2002**, *124*, 3842–3843. (b) Xu, Q.; Han, L.-B. Palladium-Catalyzed Asymmetric Hydrophosphorylation of Norbornenes. *Org. Lett.*, **2006**, *8*, 2099–2101. (c) Beaud, R.; Phipps, R. J.; Gaunt, M. J. Enantioselective Cu-Catalyzed Arylation of Secondary Phosphine Oxides with Diaryliodonium Salts toward the Synthesis of P-Chiral Phosphines. *J. Am. Chem. Soc.* **2016**, *138*, 13183–13186. (d) Nie, S.-Z.; Davison, R. T.; Dong, V. M. Enantioselective Coupling of Dienes and Phosphine Oxides. *J. Am. Chem. Soc.* **2018**, *140*, 16450–16454. (e) Trost, B. M.; Spohr, S. M.; Rolka, A. B.; Kalnins, C. A. Desymmetrization of Phosphinic Acids via Pd-Catalyzed Asymmetric Allylic Alkylation: Rapid Access to P-chiral Phosphinates. *J. Am. Chem. Soc.* **2019**, *141*, 14098–14103. (f) Yang, Z.; Gu, X.; Han, L.-B.; Wang, J. Palladium-catalyzed asymmetric hydrophosphorylation of alkynes: facile access to P-stereogenic phosphinates. *Chem. Sci.* **2020**, *11*, 7451–7455. (g) Dai, Q.; Liu, L.; Qian, Y.; Li, W.; Zhang, J.-L. Construction of P-Chiral Alkenylphosphine Oxides through Highly Chemo-, Regio-, and Enantioselective Hydrophosphinylation of Alkynes. *Angew. Chem., Int. Ed.* **2020**, *59*, 20645–20650. (h) Yang, Z.; Wang, J. Enantioselective Palladium-Catalyzed Hydrophosphinylation of Allenes with Phosphine Oxides: Access to Chiral Allylic Phosphine Oxides. *Angew. Chem., Int. Ed.* **2021**, *60*, 27288–27292. (i) Zhang, Q.; Liu, X.-T.; Wu, Y.; Zhang, Q.-W. Ni-Catalyzed Enantioselective Allylic Alkylation of H-Phosphinates. *Org. Lett.* **2021**, *23*, 8683–8687. (j) Li, B.; Liu, M.; Rehman, S. U.; Li, C. Rh-Catalyzed Regio- and Enantioselective Allylic Phosphinylation. *J. Am. Chem. Soc.* **2022**, *144*, 2893–2898. (k) Wang, H.; Qian, H.; Zhang, J.; Ma, S. Catalytic Asymmetric Axially Chiral Allenyl C-P Bond Formation. *J. Am. Chem. Soc.* **2022**, *144*, 12619–12626. (l) Alnasleh, B. K.; Sherrill, W. M.; Rubin, M. Palladium-Catalyzed Hydrophosphorylation and Hydrophosphinylation of Cyclopropenes. *Org. Lett.*, **2008**, *10*, 3231–3234.

[15] Li, Z.-Y.; Peng, G.-C.; Zhao, J.-B.; Zhang, Q. Catalytically Generated Allyl Cu(I) Intermediate via Cyclopropene Ring-Opening Coupling en Route to Allylphosphonates. *Org. Lett.* **2016**, *18*, 4840–4843.

[16] (a) Bullock, R. M.; Chen, J. G.; Gagliardi, L.; Chirik, P. J.; Farha, O. K.; Hendon, C. H.; Jones, C. W.; Keith, J. A.; Klosin, J.; Minter, S. D.; Morris, R. H.; Radosevich, A. T.; Rauchfuss, T. B.; Strotman, N. A.; Vojvodic, A.; Ward, T. R.; Yang, J. Y.; Surendranath, Y. Using Nature's Blueprint to Expand Catalysis with Earth-abundant Metals. *Science*, **2020**, *786*, 1–10. (b) Chen, J.; Lu, Zhan. Asymmetric

Hydrofunctionalization of Minimally Functionalized Alkenes via Earth Abundant Transition Metal Catalysis. *Org. Chem. Front.*, **2018**, *5*, 160–272. (c) Toutov, A. A.; Liu, W.; Betz, K. N.; Fedorov, A.; Stoltz, B. M.; Grubbs, R. H. Silylation of C-H Bonds in Aromatic Heterocycles by an Earth-abundant Metal Catalysis. *Nature*, **2015**, *518*, 80–84.

[17] (a) Fortman, G. C.; Slawin, A. M. Z.; Nolan, S. P. A Versatile Cuprous Synthone: [Cu(IPr)(OH)] (IPr = 1,3-bis(diisopropylphenyl)imidazol-2-ylidene). *Organometallics* **2010**, *29*, 3966–3972. (b) Najafabadi, B. K.; Corrigan, J. F. Enhanced Thermal Stability of Cu-Silylphosphido Complexes via NHC Ligation. *Dalton Trans.* **2015**, *44*, 14235–14241. (c) Wang, G.; Gibbons, S. K.; Glueck, D. S.; Sibbald, C.; Fleming, J. T.; Higham, L. J.; Rheingold, A. L. Copper-Phosphido Intermediates in Cu(IPr)-Catalyzed Synthesis of 1-Phosphapyracenes via Tandem Alkylation/Arylation of Primary Phosphines. *Organometallics* **2018**, *37*, 1760–1772. (d) Gibbons, S. K.; Valleau, C. R. D.; Peltier, J. L.; Cain, M. F.; Hughes, R. P.; Glueck, D. S.; Golen, J. A.; Rheingold, A. L. Diastereoselective Coordination of P-Stereogenic Secondary Phosphines in Copper(I) Chiral Bis(phosphine) Complexes: Structure, Dynamics, and Generation of Phosphido Complexes. *Inorg. Chem.* **2019**, *58*, 8854–8865. (e) Gallant, S. K.; Tipker, R. M.; Glueck, D. S. Copper-Catalyzed Asymmetric Alkylation of Secondary Phosphines via Rapid Pyramidal Inversion in P-Stereogenic Cu-Phosphido Intermediates. *Organometallics*, **2022**, *41*, 1721–1730. (f) Moncarz, J. R.; Laritcheva, N. F.; Glueck, D. S. Palladium-Catalyzed Asymmetric Phosphination: enantioselective synthesis of a P-chirogenic Phosphine. *J. Am. Chem. Soc.* **2002**, *124*, 13356–13357. (g) Blank, N. F.; Moncarz, J. R.; Brunker, T. J.; Scriban, C.; Anderson, B. J.; Amir, O.; Glueck, D. S.; Zakharov, L. N.; Golen, J. A.; Incarvito, C. D.; Rheingold, A. L. Palladium-Catalyzed Asymmetric Phosphination. Scope, Mechanism, and Origin of Enantioselectivity. *J. Am. Chem. Soc.* **2007**, *129*, 6847–6858. (h) Chan, V. S.; Stewart, I. C.; Bergman, R. G.; Toste, F. D. Asymmetric Catalytic Synthesis of P-Stereogenic Phosphines via a Nucleophilic Ruthenium Phosphido Complex. *J. Am. Chem. Soc.* **2006**, *128*, 2786–2787. (i) Chan, V. S.; Bergman, R. G.; Toste, F. D. Pd-Catalyzed Dynamic Kinetic Enantioselective Arylation of Silylphosphines. *J. Am. Chem. Soc.* **2007**, *129*, 15122–15123. (j) Chan, V. S.; Chiu, M.; Bergman, R. G.; Toste, F. D. Development of Ruthenium Catalysts for the Enantioselective Synthesis of P-Stereogenic Phosphines via Nucleophilic Phosphido Intermediates. *J. Am. Chem. Soc.* **2009**, *131*, 6021–6032.

[18] Deposition number 2100976 for **3aa** and 2154097 for **4ja**, contains the supplementary crystallographic data for this paper. These data are provided free of charge by the joint Cambridge Crystallographic Data Centre and Fachinformationszentrum Karlsruhe Access Structures service www.ccdc.cam.ac.uk/structures. The absolute configurations of the remaining cyclopropyl phosphine sulfides **3** are assigned by analogy.

[19] Xu, P.-W.; Yu, J.-S.; Chen, C.; Cao, Z.-Y.; Zhou, F.; Zhou, J. Catalytic Enantioselective Construction of Spiro Quaternary Carbon Stereocenters. *ACS Catal.* **2019**, *9*, 1820–1882.

[20] Rios, R. Enantioselective methodologies for the synthesis of spiro compounds. *Chem. Soc. Rev.* **2012**, *41*, 1060–1074.

[21] (a) Edwards, A.; Rubina, M.; Rubin, M. Nucleophilic Addition of Cyclopropenes. *Curr. Org. Chem.* **2016**, *20*, 1862–1877. (b) Fox, J. M.; Yan, N. Metal Mediated and Catalyzed Nucleophilic Additions to Cyclopropenes. *Curr. Org. Chem.*, **2005**, *9*, 719–732. (c) Alnasleh, B. M.; Sherrill, W. M.; Rubina, M.; Banning, J.; Rubin, M. Highly Diastereoselective Formal Nucleophilic Substitution of Bromocyclopropanes. *J. Am. Chem. Soc.* **2009**, *131*, 6906–6907.

[22] (a) Ananikov, V. P.; and Beletskaya, I. P. Alkyne Insertion into the M-P and M-H Bonds (M = Pd, Ni, Pt, and Rh): A Theoretical Mechanistic

- Study of the C-P and C-H Bond Formation Steps. *Chem. Asian J.* **2011**, *6*, 1423–1430. (b) Burton, K. M. E.; Pantazis, D. A.; Belli, R. G.; McDonald, R.; Rosenberg, L. Alkene Insertion into a Ru-PR₂ Bond. *Organometallics* **2016**, *35*, 3970–3980.
- [23] Zall, C. M.; Linehan, J. C.; Appel, A. M. Triphosphine-Ligated Copper Hydrides for CO₂ Hydrogenation: Structure, Reactivity, and Thermodynamic Studies. *J. Am. Chem. Soc.* **2016**, *138*, 9968–9977.
- [24] Yamamoto, Y. Theoretical Study of the Copper-Catalyzed Hydroarylation of (Trifluoromethyl)alkyne with Phenylboronic Acid. *J. Org. Chem.* **2018**, *83*, 12775–12783
- [25] Steinreiber, J.; Faber, K.; Griengl, H. De-racemization of Enantiomers versus De-epimerization of Diastereomers—Classification of Dynamic Kinetic Asymmetric Transformation (DYKAT). *Chem. Eur. J.* **2008**, *14*, 8060–8072.
- [26] Buhro, W. E.; Zwick, B. D.; Georgiou, S.; Hutchinson, J. P.; Gladysz, J. A. Synthesis, Structure, Dynamic Behavior, and Reactivity of Rhenium Phosphido Complexes ([⁵-C₂H₅)Re(NO)(PPh₃)(PR₂): The “Gauche Effect” in Transition-Metal Chemistry. *J. Am. Chem. Soc.* **1988**, *110*, 2427–2439.
- [27] Chai, J. D.; Head-Gordon, M. Long-range corrected hybrid density functionals with damped atom-atom dispersion corrections. *Phys. Chem. Chem. Phys.* **2008**, *10*, 6615–6620.
- [28] Grimme, S. Semiempirical GGA-type density functional constructed with a long-range dispersion correction. *J. Comput. Chem.* **2006**, *27*, 1787–1799.
- [29] Becke, A. Density-Functional Thermochemistry. V. Systematic Optimization of Exchange-Correlation Functionals. *J. Chem. Phys.* **1997**, *107*, 8554–8560.
- [30] Weigend, F.; Ahlrichs, R. Balanced basis sets of split valence, triple zeta valence and quadruple zeta valence quality for H to Rn: Design and assessment of accuracy. *Phys. Chem. Chem. Phys.* **2005**, *7*, 3297–3305.
- [31] Miertus, S.; Scrocco, E.; Tomasi, J. Electrostatic Interaction of a Solute with a Continuum - a Direct Utilization of Abinitio Molecular Potentials for the Prevision of Solvent Effects. *Chem. Phys.* **1981**, *55*, 117–129.
- [32] Tomasi, J.; Mennucci, B.; Cammi, R. Quantum mechanical continuum solvation models. *Chem. Rev.* **2005**, *105*, 2999–3093.
- [33] Frisch, M. J.; Trucks, G. W.; Schlegel, H. B.; Scuseria, G. E.; Robb, M. A.; Cheeseman, J. R.; Scalmani, G.; Barone, V.; Petersson, G. A.; Nakatsuji, H.; Li, X.; Caricato, M.; Marenich, A. V.; Bloino, J.; Janesko, B. G.; Gomperts, R.; Mennucci, B.; Hratchian, H. P.; Ortiz, J. V.; Izmaylov, A. F.; Sonnenberg, J. L.; Williams; Ding, F.; Lipparini, F.; Egidi, F.; Goings, J.; Peng, B.; Petrone, A.; Henderson, T.; Ranasinghe, D.; Zakrzewski, V. G.; Gao, J.; Rega, N.; Zheng, G.; Liang, W.; Hada, M.; Ehara, M.; Toyota, K.; Fukuda, R.; Hasegawa, J.; Ishida, M.; Nakajima, T.; Honda, Y.; Kitao, O.; Nakai, H.; Vreven, T.; Throssell, K.; Montgomery, J. A., Jr.; Peralta, J. E.; Ogliaro, F.; Bearpark, M. J.; Heyd, J. J.; Brothers, E. N.; Kudin, K. N.; Staroverov, V. N.; Keith, T. A.; Kobayashi, R.; Normand, J.; Raghavachari, K.; Rendell, A. P.; Burant, J. C.; Iyengar, S. S.; Tomasi, J.; Cossi, M.; Millam, J. M.; Klene, M.; Adamo, C.; Cammi, R.; Ochterski, J. W.; Martin, R. L.; Morokuma, K.; Farkas, O.; Foresman, J. B.; Fox, D. J. *Gaussian 16*; Rev. C.01: Wallingford, CT, 2016.
- [34] Ribeiro, R. F.; Marenich, A. V.; Cramer, C. J.; Truhlar, D. G. Use of solution-phase vibrational frequencies in continuum models for the free energy of solvation. *J. Phys. Chem. B* **2011**, *115*, 14556–14562.
- [35] O’Duill, M. L.; Engle, K. M. Protodepalladation as a Strategic Elementary Step in Catalysis. *Synthesis*, **2018**, *50*, 4699–4714.
- [36] Yao, Y.; Zhang, X.; Ma, S. DFT study on the E-stereoselective reductive A³-coupling reaction of terminal alkynes with aldehydes and 3-pyrroline. *Org. Chem. Front.*, **2020**, *7*, 2047–2054.
- [37] Yuan, X.; Wang, S.; Jiang, Y.; Liu, P.; Bi, S. Distinctive mechanistic scenarios and substituent effects of gold(I) versus copper(I) catalysis for hydroacylation of terminal alkynes with glyoxal derivatives. *J. Am. Chem. Soc.* **2022**, *87* (17), 11681–11692.
- [38] Bickelhaupt, F. M.; Houk, K. N., Analyzing Reaction Rates with the Distortion/Interaction-Activation Strain Model. *Angew. Chem. Int. Ed. Engl.* **2017**, *56* (34), 10070–10086.
- [39] Ess, D. H.; Houk, K. N., Distortion/interaction energy control of 1,3-dipolar cycloaddition reactivity. *J. Am. Chem. Soc.* **2007**, *129* (35), 10646–7.
- [40] Maji, R.; Mallojjala, S. C.; Wheeler, S. E., Chiral phosphoric acid catalysis: from numbers to insights. *Chem. Soc. Rev.* **2018**, *47* (4), 1142–1158
- [41] Lu, T.; Chen, Q., Independent gradient model based on Hirshfeld partition: A new method for visual study of interactions in chemical systems. *J. Comput. Chem.* **2022**, *43* (8), 539–555.
- [42] Lu, T.; Chen, F. Multiwfn: A multifunctional wavefunction analyzer. *J. Comput. Chem.* **2011**, *33* (5), 580–592.
- [43] Falivene, L., Cao, Z., Petta, A.; Serra, L.; Poater, A.; Oliva, R.; Scarano, V.; Cavallo, L. Towards the online computer-aided design of catalytic pockets. *Nat. Chem.* **2019**, *11*, 872–879.
- [44] Schaefer, A. J., Ingman, V. M., Wheeler, S. E. SEQCROW: A ChimeraX bundle to facilitate quantum chemical applications to complex molecular systems. *J. Comput. Chem.* **2021**, *42* (24), 1750–1754.
- [45] There is little difference between the buried volumes of L3 and L4, corresponding with the little difference in the observed ee for L3 and L4 (see Supplementary Information Table S2 for buried volumes and all steric maps).